Molecular physisorption on graphene and carbon nanotubes:

A comparative *ab initio* study

Daniel Henwood [a)] and J David Carey [b)]

Advanced Technology Institute, University of Surrey,

Guildford, GU2 7XH, United Kingdom.

Abstract

The results of *ab initio* density functional theory calculations of molecular physisorption on a number of different adsorption sites on a graphene sheet and on a (10, 0) single walled carbon nanotube are discussed. Both the Vosko-Wilk-Nusair (VWN) local density approximation (LDA) functional and the Perdew-Wang (PW91) generalized gradient approximation (GGA) functional were employed in calculating the binding energy of a hydrogen molecule to the appropriate carbon nanostructure as well as the optimal molecule – nanostructure separation. Both exterior and interior nanotube adsorption sites were examined and it is shown that the binding energy associated with interior adsorption sites is larger than exterior adsorption on the nanotube or onto the graphene layer. The use of carbon nanostructures for hydrogen storage is also discussed.

Keywords: graphene, carbon nanotube, hydrogen, physisorption, LDA and GGA functionals

a) Email: D.Henwood@surrey.ac.uk

b) Email: David.Carey@surrey.ac.uk

1. Introduction

Ab initio calculations play a crucial role in attempting to understand many of the electronic properties of a material with density functional theory (DFT) being one of the common approaches to calculating material properties [1]. The field of nanomaterials continues to expand with new materials and new structures of existing materials being continually reported. Often *ab initio* calculations can provide predictions which can be tested by experiment which, in turn inform and refine the calculations. In the case of carbon based nanomaterials the confirmation of the structure of one dimensional single walled carbon nanotubes [2] in 1991 and the recent production of a stable two dimensional layer of graphene [3] in 2004 have brought about a dual renaissance in research into carbon as an electronic material [4]. Carbon nanotubes (CNTs), both the single-walled and multi-walled varieties, have emerged as the leading new nanomaterial and in terms of potential applications have already found use as electron field emitters [5] and in gas sensing [6]. In both cases *ab initio* studies have, for example, been employed to examine how the frontier (HOMO and LUMO) orbitals are affected by the presence of large electric fields found in field emission [7, 8] or how the presence of an adsorbed molecule with a different ionization potential may result in electron donation or withdrawal [9].

The potentially large surface area of CNTs has also led to the possibility of the use of CNTs in gas storage, in particular for hydrogen storage [10]. Whilst a range of different approaches, such as solid-state storage using metal hydrides [11] are being investigated, it is worth highlighting that in addition to a high storage capability, efficient delivery of the gas is also a crucial parameter. While hydrogen chemisorption could provide a route to a higher amount of hydrogen which can be absorbed, desorption would need to take place at temperatures in excess of 600 K which is not desirable from a technological viewpoint [12]. To that end a study of the physisorption of H_2 is important since the typical binding energies are less than chemisorption as only relatively weak van der Waals (vdW) interactions are present. A knowledge of the binding energy can then be used in conjunction with the van't Hoff equation [13] to estimate the desorption temperature.

The tubular nature of CNTs can potentially lend themselves to storage on both the interior as well as a range of different exterior sites and as a consequence knowledge of possible binding sites for internal and external adsorption is required. The emergence of graphene, consisting of a stable hexagonal sheet of sp^2 bonded carbon atoms, is also a significant milestone in carbon nanomaterials. As the hexagonal plate of graphene can be regarded as the building block of CNTs the adsorption of gases on graphene is an important topic and has itself become the subject of extensive research with the recent report of single molecule detection on a stable layer of graphene [14].

It is important to point out at this stage that there are different possible approaches to the study of molecular physisorption with DFT being only one. DFT is well known to have limitations in accurately representing the long range van der Waals interactions. There is a general acceptance [1] that the electron exchange and correlation interactions are not well represented by either the local density approximation (LDA) or the generalized gradient approximation (GGA). As a result the use of the former approximation tends to result in an over estimation of the binding energy between molecules and an under estimation of the optimum intermolecular separation. In the case of the GGA, the reverse is true with an underestimation of the binding energies. However, both the LDA and GGA are excellent starting points for the calculation of binding energies and the trends between and values of the binding energy associated for different sites can give the important information. In doing so, however, care should be exercised in placing over emphasis on the exact values obtained. Alternative methods such as Monte Carlo based methods or molecular orbital methods are also employed but they themselves have intrinsic limitations in modelling both solids and the gas phase and/or are computationally expensive. Furthermore beyond the atomistic methods there is modelling on the larger scale where the competing effects of kinetics and thermodynamics of adsorption and desorption also need to be considered. As a result a wide range of approaches from DFT to more sophisticated methods should be considered. In this paper the physisorption of hydrogen on a range of different sites on a graphene sheet as well as on a (10, 0) single walled carbon nanotube will be investigated using both the local density approximation (LDA) and the generalized gradient approximation (GGA).

2. Simulation details

Density functional theory calculations were performed using the DMol^3 code within the Materials Studio modeling suite [15] employing a double numerical with polarization basis set (DNP). The efficiency of this basis set has recently being examined in detail [16] for hydrogen and carbon and compared with other basis sets and found to be of sufficient in terms of a negligible basis set superposition error. In the case of adsorption on graphene, a hexagonal plate of 96 sp^2 bonded carbon atoms was chosen [17]. The bond lengths for the graphene layer were 0.142 nm which agrees with the experimental values of 0.141 nm. Figure 1a shows a segment of the graphene layer and the different adsorption sites. In sites A - C the hydrogen molecular axis is oriented perpendicular to the graphene layer, whereas in sites D - F the hydrogen molecular axis lies parallel to the graphene layer. For the simulations of the CNT, a segment consisting of 120 carbon atoms was used. This length was chosen as it was found that hydrogen adsorption was affected by the terminating hydrogen atoms for shorter segments of nanotube. The H_2 bond length was 0.074 nm. For calculations within the LDA, the Vosko-Wilk-Nusair (VWN) functional was used and for the GGA approximation the Perdew-Wang (PW91) functional was employed. The separation between the hydrogen center-of-mass and the carbon nanostructure (graphene layer or nanotube wall as appropriate) was varied systematically and the potential energy (E_b) was calculated from

$$E_b = E_{nano\text{-}H_2} - E_{nano} - E_{H_2} \tag{1}$$

where $E_{nano\text{-}H_2}$ is the energy of the hydrogen and carbon nanostructure (graphene or nanotube) system, E_{nano} is the energy of the nanostructure on its own and E_{H_2} is the energy of the hydrogen molecule. The minimum in equation (1) is the binding energy of the H_2 to the nanostructure.

3. Adsorption on Graphene and Carbon Nanotubes

In the case of graphene, the variation of potential energy with separation for adsorption at site D given in Fig. 1a is shown in Fig. 2 for both functionals under investigation. Calculations with the LDA

VWN functional give a binding energy of 93 meV at an intermolecular separation of 0.27 nm which is similar to the value of 86 meV reported by Arellano *et al.* [18]. Calculations with the PW91 GGA functional show a lower binding energy of 23 meV with an optimum separation of 0.33 nm. The interaction energy curves displayed in Fig. 2 show the typical form of a Lennard-Jones potential: an attractive region at medium separation that turns and becomes repulsive at short intermolecular separations. At large intermolecular separations the interaction energy tends to zero but grows steadily more negative (attractive) as the hydrogen molecule is brought closer to the graphene plate. As the hydrogen molecule passes the binding energy minima, the Pauli repulsion interactions start to dominate and the interaction energy starts to climb. As the separation between the hydrogen and graphene molecule decreases, electrons in the σ molecular orbital of the H_2 start to overlap with electrons in the π state of the graphene. This has the effect of forming bonding and anti-bonding states between the two molecules. The repulsive force that develops from the rise in the energy of the filled anti-bonding state pushes the molecules apart forming an energy barrier. If the structure of the molecules was allowed to relax, as the hydrogen approaches the graphene plate, the height of the barrier would become finite as the increase in the system energy would be enough to overcome the covalent bond of the hydrogen molecule. This is due to the rise of the filled molecular anti-bonding state to a level above the unfilled, anti-bonding state of the hydrogen molecule. The electrons in the anti-bonding molecular orbital would drop into the lower energy, anti-bonding state of the hydrogen molecule with the result that the hydrogen molecule would dissociate and form C-H bonds with the π state electrons in the delocalised graphitic ring.

Similar potential energy curves have been found for the other sites on the graphene layer as well as on the corresponding sites (Fig. 1b) on the (10, 0) CNT. Figure 3 shows the binding energies for all the sites investigated in Figure 1 and the corresponding internal sites in the case of the carbon nanotubes using both the LDA (Fig. 3a) and the GGA (Fig. 3b) functionals. In the case of the adsorption modeled using the local density approximation it can be seen that for all sites investigated the lowest binding energy was found on the exterior surface of the nanotube with typical binding

energies in the range of 60 – 80 meV with the hydrogen molecular axis perpendicular to the nanotube. Slightly higher binding energies (85 – 90 meV) are found exterior to the CNT with the H_2 axis parallel to the nanotube. Adsorption on graphene in the corresponding sites appears to be slightly more favourable by about 10 – 15 meV. The highest binding energies are found for internal adsorption where the most favourable cases have binding energies of around 150 meV. Again it would appear that parallel configurations (D – G) of H_2 are slightly more favoured than perpendicular ones; though care must be used in looking at the absolute values of the binding energies due to the inherent difficulties with the van der Waals interactions. The corresponding binding energies calculated using the generalized gradient approximation show much smaller binding energies of around 20 - 22 meV and 23 meV for adsorption on the exterior wall of the nanotube and the graphene layer, respectively. The binding energy on the interior surface of the nanotube is around 50 meV for all sites. The two main conclusions that can be drawn from these results are that there is no one favoured site for physisorption on the exterior surface of nanotubes and graphene and that the binding energy associated with adsorption on the interior surface is larger than the exterior surface. In addition charge density plots, not shown here, show no evidence of significant charge transfer [16].

The absence of preferred sites for physisorption is not just limited to carbon based materials. DFT calculations have also been carried out on other sp^2 graphitic materials such as BN. Jhi and Kwon showed that H_2 adsorbs on a hexagonal BN (*h*BN) sheet with a binding energy of about 90 meV with little difference between the hexagonal site (equivalent to site B in Fig. 1a) and adsorption over a boron or nitrogen site [19]. They further went onto study a carbon doped BN sheet where the binding energy increased to about 125 meV for carbon at a boron substitutional site and about 100 meV for carbon at a nitrogen substitutional site. For BN nanotubes, binding energies of between 85 and 110 meV were observed for different sites.

4. Modification of the MO energies

Whilst physisorption does not form chemical bonds it does not mean that there are no changes to the molecular orbitals of the molecules. In particular there is considerable interest in any changes to the frontier orbitals (HOMO and LUMO) when molecules are physisorbed. This is a particularly important area in organic electronics when molecules are placed in contact with metal contacts. Upon adsorption there appears as a reduction to the ionization potential (IP) and an increase in the electron affinity (EA) of the adsorbed molecule when compared with the isolated molecule. For example, Neaton *et al*. in a recent study of the adsorption of benzene on graphite (0001) using the GW approximation found that the gas phase HOMO-LUMO gap for benzene of 10.5 eV was reduced to 7.2 eV on physisorption onto the graphite surface [20]. It was found that there exists a near (but opposite in direction) shift of about 1.50 eV and –1.43 eV for the HOMO and LUMO levels of benzene, respectively. The origin of these energy shifts is consistent with a surface polarization effect and a classical image charge was able to account for their magnitude. They further showed that nearly equal shifts of the frontier orbitals were possible for a range of hydrocarbons on graphite with polarization energies between 1.2 to 1.4 eV.

Figure 4 shows the variation of the HOMO level for the H_2 on adsorption to graphene using both the LDA and GGA approaches. It can be seen that the HOMO level rises up as the H_2 – graphene separation reduces. The value of the HOMO level for the isolated H_2 molecule is -10.24 eV using LDA and -10.41 eV using GGA and the calculated value of the LUMO level is 1.60 eV and 1.66 eV, respectively. It should be noted that as the separation increases the value of the HOMO level converges to the calculated isolated value. As a result the isolated HOMO-LUMO separation is 11.84 eV and 12.07 eV, using LDA and GGA, respectively. Figure 4 shows the shift of the HOMO level where it can be observed that at the optimum binding energy separation calculated by the PW91 functional, the HOMO level has reached -10.0 eV, representing a 0.4 eV change. Similarly for the optimum site determined by the LDA method the HOMO level has reached -9.85 eV, an almost identical shift of 0.39 eV. While these shifts are almost the same, the behavior of the HOMO levels

differs at very short intermolecular separation with a continued decrease calculated by GGA and a levelling off and then slight increase to more negative values seen by LDA. The reasons for the different behaviour are unclear at this stage. For practical reasons [21] we are unable to monitor the variation of the LUMO level but on the basis that there is an equal shift of 0.4 eV in the LUMO level, an estimate of the HOMO-LUMO separation on adsorption is now reduced by 0.8 eV to 11.05 eV (LDA) and 11.26 eV (GGA). For adsorption on metals an image charge method is often employed and to induce a shift of 0.4 eV would require the H_2 molecule to be located around 0.9 nm from the surface. This is clearly not at the bottom of the potential well, as seen in Fig. 2, and would suggest that further exploration is needed to resolve this change in particular by using alternative methods to LDA and GGA.

In summary DFT calculations have been used to examine the optimum binding energy and position of hydrogen physisorption to graphene and to a (10, 0) carbon nanotube. It is found that the highest binding energy is in the interior of the nanotube but there does not appear to exist a preferential site with all sites investigated appearing to produce comparable binding energies. We have also examined the behaviour of the highest occupied molecular orbital on adsorption and conclude that there is a 0.8 eV reduction of the HOMO-LUMO gap of H_2 on adsorption on graphene.

Acknowledgment The authors would like to thank the EPSRC (UK) for funding.

References

[1] See, for example, Springer Series, Lecture Notes in Physics, vol. **620**, *A Primer in Density Functional Theory*, ed. C. Fiolhais, F. Nogueira and M.A.L. Marques (2003).

[2] S Iijima, *Nature* **354**, 56 (1991).

[3] K. S. Novoselov, D. Jiang, F. Schedin, T. J. Booth, V. V. Khotkevich, S. V. Morozov, and A. K. Geim, Proc. Natl. Acad. Sci. **102**, 10451 (2005).

[4] Springer series, Topics in Applied Physics, vol. **100**, *Carbon: The Future Marterial for Advanced Technology Applications*, ed. G. Messina and S. Santangelo (2006).

[5] K.B.K. Teo, E. Minoux, L. Hudanski, F. Peauger, J.-P. Schnell, L. Gangloff, P. Legagneux, D. Dieumgard, G.A.J. Amaratunga and W.I. Milne. Nature **437**, 968 (2005)

[6] P. G. Collins, K. Bradley, M. Ishigami, A. Zettl, Science **287**, 1801 (2000).

[7] M. Khazaei and Y. Kawazoe, Surface Science **601**, 1501 (2007).

[8] A. Maiti, J. Andzelm, N. Tanpipat and P. von Allmen, Phys. Rev. Lett. **87**, 155502 (2001).

[9] S-H Jhi, S. G. Louie, and M. L. Cohen, Phys. Rev. Lett. **85**, 1710 (2000).

[10] M. S. Dresselhaus, *Basic Research Needs for the Hydrogen Economy*, 2nd ed. Office of Basic Energy Sciences, U.S. Department of Energy, Washington, DC, (2004).

[11] B. Bogdanović and G. Sandrock, MRS Bull. **27**, 712 (2002)

[12] S. K. Bhatia and A. L. Myers, Langmuir **22**, 1688 (2006).

[13] See, for example, Physical Chemistry, P.W. Aitken, 8th edition, chapter 8. (Oxford).

[14] F. Schedin, A. K. Geim, S. V. Morozov, E. W. Hill, P. Blake, M. I. Katsnelson & K. S. Novoselov, Nature Materials **6**, 652 (2007)

[15] B. Delly, J. Chem. Phys **92**, 508 (1990); J. Quant. Chem. **69**, 423 (1998).

[16] Yasuji Inada, Hideo Orita, J Comput. Chem. **29**, 225 (2008).

[17] D. Henwood and J. David Carey, Phys. Rev. B **75**, 245413 (2007).

[18] J. S. Arellano, L. M. Molina, A. Rubio and J. A. Alonso, J. Chem. Phys. **112**, 8114 (2000).

[19] S-H Jhi and Y-K Kwon, Phys. Rev B **69**, 245407 (2004).

[20] J.B. Neaton, M.S. Hybertsen and S. G. Louie, Phys. Rev. Lett. **97**, 216405 (2006).

[21] The software is only able to provide data on the first 10 LUMO levels and the unoccupied MO level associated with the introduction of the H_2 molecules lies outside of the 10 levels. Hence we are unable to monitor its position.

Figure captions

Figure 1 Possible hydrogen physisorption sites on a segment (a) of graphene and (b) the exterior surface of a (10, 0) single walled carbon nanotube.

Figure 2 Potential energy curve of hydrogen physisorption on graphene in site D using both VWN LDA (○) and PW91 GGA (●) functionals.

Figure 3 Binding energies of hydrogen physisorption on graphene (■) and both the interior (●) and exterior (○) sites for using (a) VWN LDA functional and (b) PW91 GGA functional. Sites A - C correspond to the hydrogen molecular axis oriented perpendicular to the graphene or nanotube surface, whereas D - G are with the hydrogen molecular axis oriented parallel to the surface.

Figure 4 Variation of the HOMO level with intermolecular separation using the (a) VWN LDA functional (○) and (b) PW91 GGA functional (●).

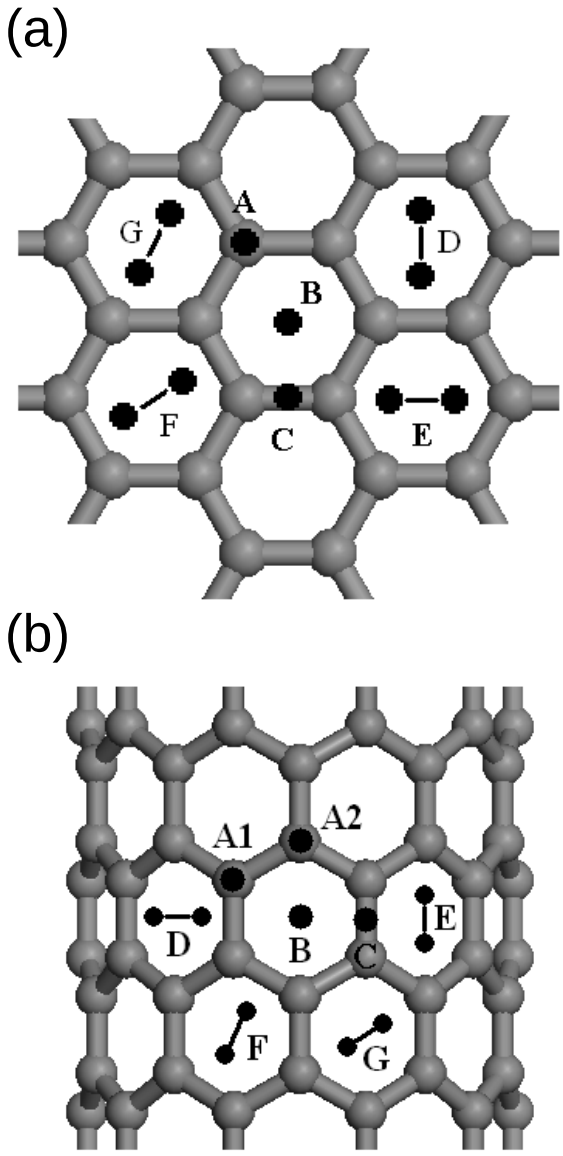

Figure 1. Henwood and Carey

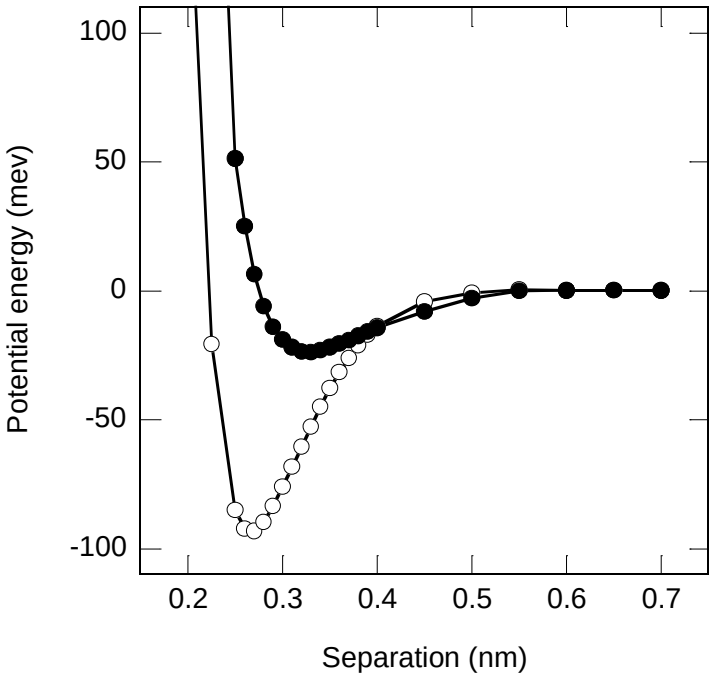

Figure 2. Henwood and Carey

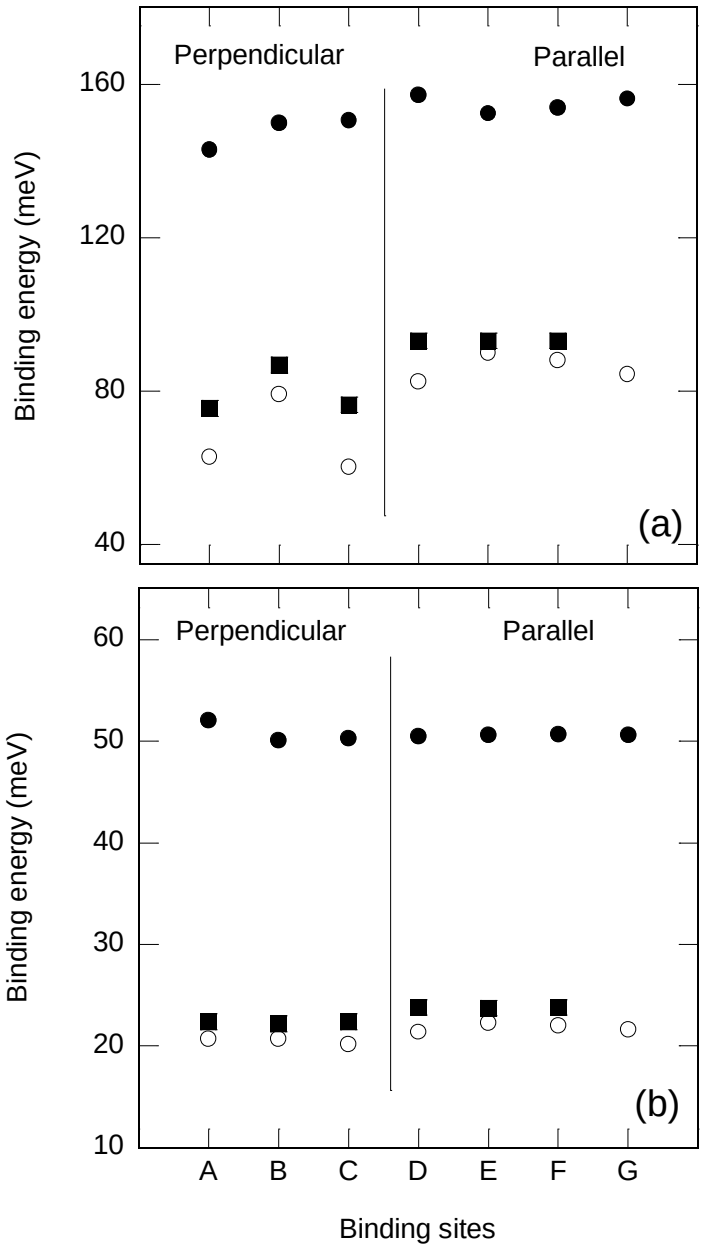

Figure 3, Henwood and Carey

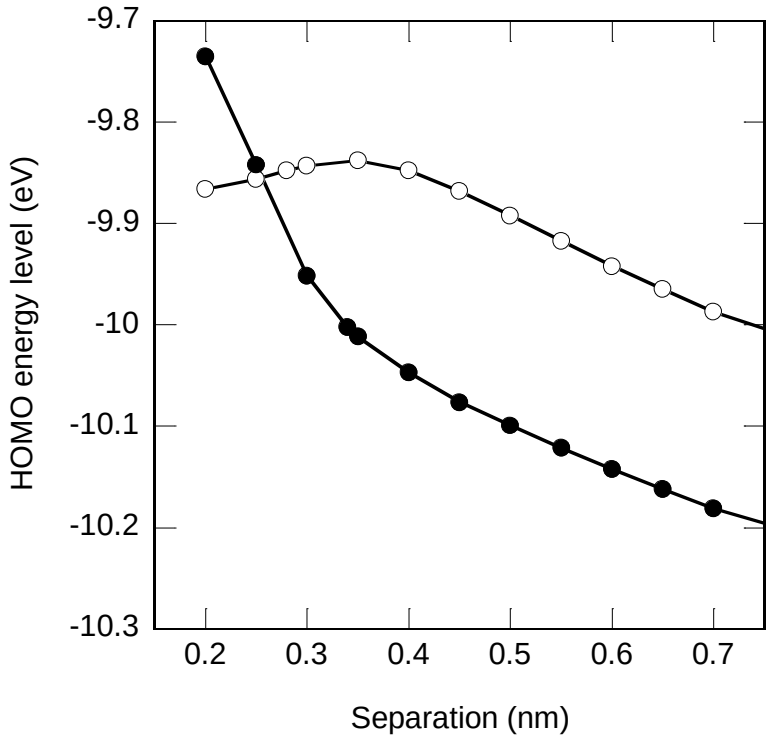

Figure 4 Henwood and Carey